M. D. COUSINS, R. C. LIVINGSTON, C. L. RINO, and J. F. VICKREY

THE HILAT SATELLITE MULTIFREQUENCY RADIO BEACON

The HILAT beacon, L-band/UHF antenna, and ground receiver system allow us to make efficient phase scintillation measurements. The L-band signal also accepts bi-phase modulated telemetry data from the other scientific instruments by means of the Science Data Formatter. Thus, the L-band signal serves the dual functions of telemetry channel and phase reference for the scintillation measurements.

BACKGROUND

The primary objective of the HILAT satellite program is to understand the physics of the large-scale electron density irregularities that cause disruptive scintillation effects on transionospheric radio signals. Irregular variations in the electron density, when sufficiently large, act like lenses that focus and defocus the radio waves, causing rapid amplitude variations (scintillation) and, ultimately, loss of frequency coherence.

Because of the lens-like action of the ionosphere, the signal phase shift near the disturbed region is proportional to the integral of the electron density evaluated along the propagation path. The amplitude variation is very small. As the wavefield propagates away from the disturbed regions, amplitude scintillation develops. Rapid phase excursions, which distort the high-frequency spectral components, accompany the signal fades. Nevertheless, for weak to moderate scintillation, the signal phase retains the main characteristics of the irregularities in the source region; moreover, the path integral is sensitive to the spatial coherence of the irregularities.

For scientific diagnostics, the signal phase is the quantity of primary interest. The spectral characteristics of the phase scintillation can be related to the corresponding spectral characteristics of the in situ irregularities. The systematic changes with changing propagation angles (relative to the direction of the earth's magnetic field) can be used to determine the spatial coherence (anisotropy) of the irregularities. Measurements with separated antennas give a more direct measure of the irregularity anisotropy.

The HILAT beacon transmits phase-coherent signals at L band, UHF, and VHF. The L-band signal is used as a phase reference to synchronously demodulate the UHF and VHF signals. Thus, the signal phase as measured at UHF, for example, is actually the difference between the UHF phase perturbation and the L-band phase perturbation divided by the ratio of the L-band frequency to the UHF frequency. For weak to moderate disturbances, the phase perturbation varies linearly with wavelength, and this effect can be readily compensated for. At VHF, the error is less than 2% and it can be ignored.

With adequate sampling, it is possible to obtain a continuous phase record for the entire pass; however, the absolute reference level is ambiguous within a multiple of 2π. To remove this ambiguity, three frequencies are transmitted at UHF. The maximum change in the expected ionospheric integrated electron content will cause less than a 2π change in the second difference of phase. Thus, the three-frequency measurement can be used to remove the 2π ambiguity.

OPERATION OF THE MULTIFREQUENCY BEACON

Table 1 lists the frequencies and radiated power of the HILAT beacon. The beacon is made up of eight modules arranged in two mounting frames as shown schematically in Fig. 1. The oscillator module contains a temperature-compensated crystal oscillator and a divider circuit for generating signals at 45.892 and 22.946 megahertz (MHz). All other signals are generated by multiplying and/or mixing the signals. For example, the UHF modulator mixes the 22.946 MHz signal with a 413.028 MHz signal (the ninth harmonic of 45.892 MHz) to generate a double sideband spectrum. The 413.028 MHz signal is reinserted to provide the three spectral lines at UHF.

The L-band modulator provides antipodal modulation of the carrier. The input is a 4098 bit per second data stream generated by the satellite science data formatter. The L-band power amplifier consists of a two-stage tuned transistor amplifier with an output of 33 decibels referenced to 1 milliwatt. This power level is sufficient to achieve the necessary link margin for good telemetry decoding.

The power supply is a simple switching type, with the switch frequency near 28 kHz and a nominal 28 volt input. Five different voltage outputs drive the beacon circuitry. With a power consumption of 20 watts, the L-band output power is 32.5 decibels referenced to 1 milliwatt. The beacon will operate from -25 to 52 °C.

Table 1—Signals transmitted by HILAT beacon.

Frequency (MHz)	*Radiated Power (decibels referenced to 1 milliwatt)*	*Purpose*
1239.084	33	Telemetry phase reference
447.447	20	Scintillation/total electron content
413.028	23	Scintillation/total electron content
378.609	20	Scintillation/total electron content
137.676	23	Scintillation

L-BAND/UHF ANTENNA

The main antenna is a nested bifilar helix structure. The bifilar helix (volute) provides a compact antenna structure with good pattern characteristics for full earth coverage. It was found that nesting the L-band helix inside a contrawound UHF helix did not affect the L-band pattern adversely; moreover, the combined structure provided good phase dispersion characteristics over the UHF frequencies. The latter property is important because the second difference of phase for the three UHF signals is used to derive an absolute measure of the path integrated electron content.

The VHF antenna is a separate "tripole" located at the tip of the x solar panel. The lack of a common phase center at VHF is not a serious problem because the phase center varies slowly over the orbit and, therefore, does not bias the more rapid phase scintillations.

A prototype of the spacecraft antenna together with the beacon electronics frames is shown in Fig. 2. The L-band volute is inside the UHF helix. The structure is 18 inches high and 4 inches square at the base.

THE GROUND RECEIVER SYSTEM

A functional diagram of the main HILAT receiving stations is shown in Fig. 3. The antenna is a four-element helix array at L band with a single UHF helix in the center. The signals are amplified at the antenna and transmitted to the scintillation receiver/demodu-

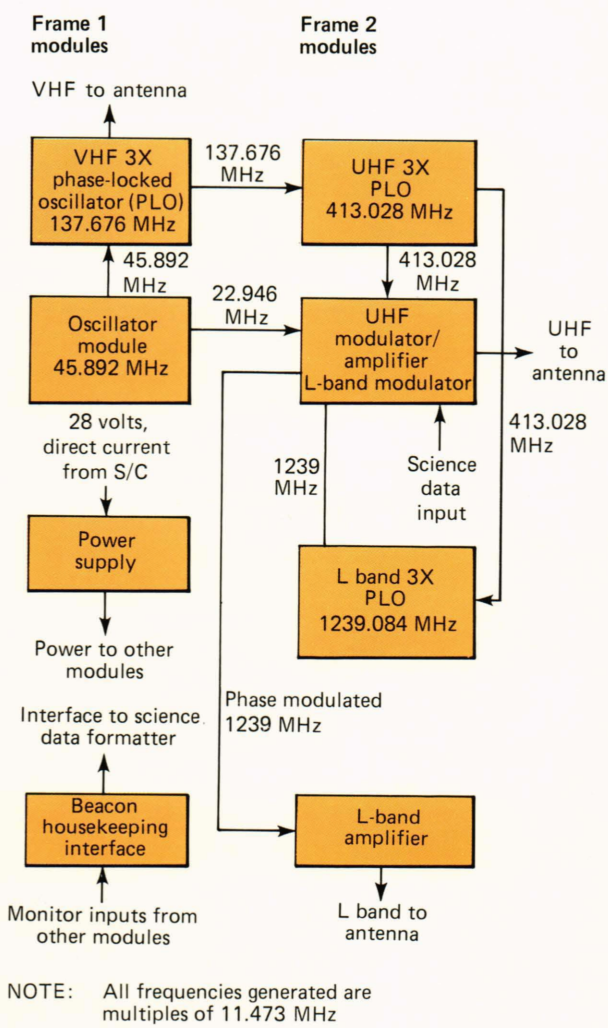

Figure 1—Functional diagram of HILAT beacon.

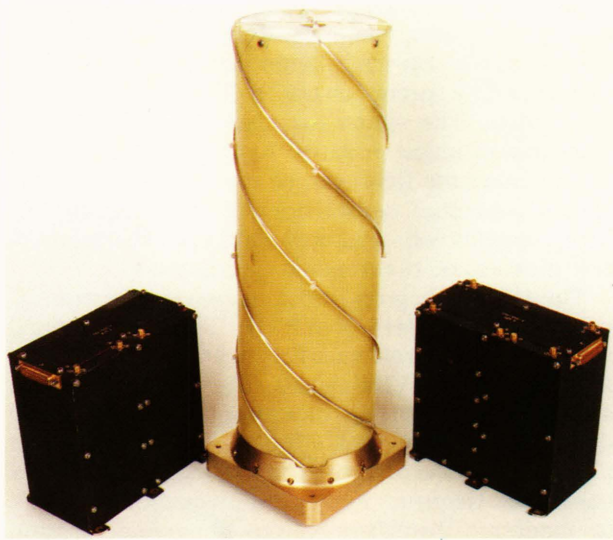

Figure 2—Prototype of beacon modules and antenna.

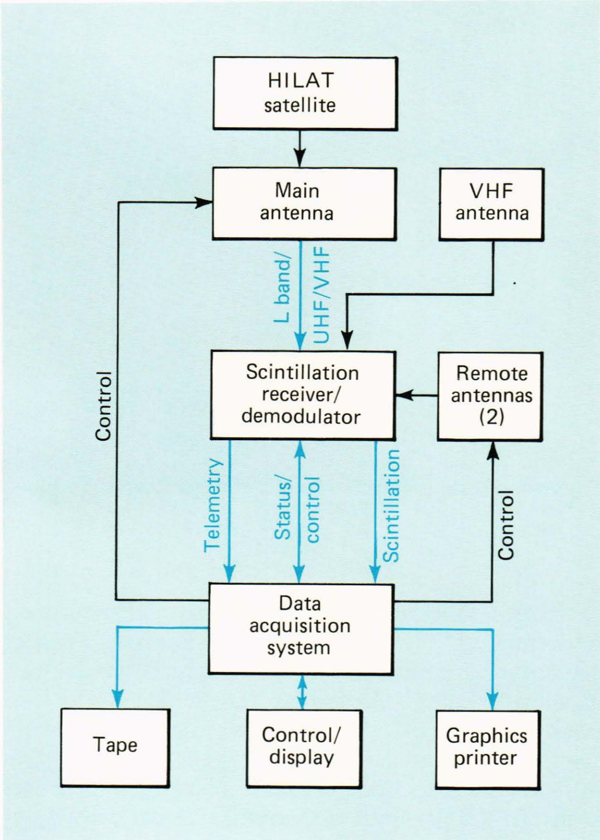

Figure 3—Diagram of HILAT ground station.

lator. An L-band carrier recovery loop is used to generate the reference signal for demodulating the telemetry data and synchronously demodulating the UHF and VHF signals.

The data acquisition system is a Hewlett-Packard A700 general-purpose computer with appropriate interfaces for transmitting control signals, receiving telemetry data, and sampling the complex scintillation channels. The computer also generates steering commands for the main L-band/UHF antenna and the UHF remote antennas. The VHF antenna is a fixed

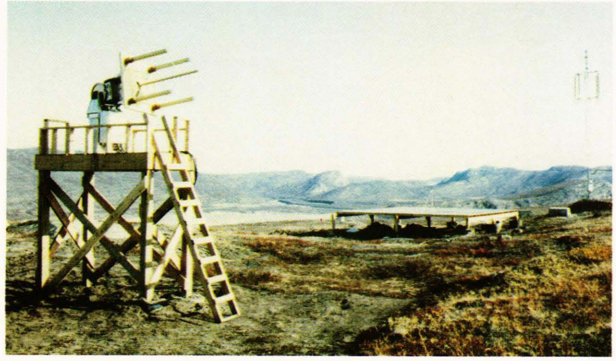

Figure 4—Main antennas at Sondre Stromfjord.

turnstile. Figure 4 is a photograph of the antenna system at the Sondre Stromfjord, Greenland, site.

Data acquisition is controlled by a scheduler that determines the times of the passes and initiates tracking and signal acquisition at the appropriate times. The data are initially recorded on a 26 megabyte hard disk but backed up on digital tape after each pass. Between passes, the scheduler initiates a data analysis program that processes all the data recorded during the pass. The storage capacity of the system is 15 to 18 passes. For routine operation it is convenient to have an operator check the station daily, which permits recording all passes that achieve a maximum elevation angle of 20° or more.

The raw data tapes and the summary tapes are being archived at the Air Force Geophysics Laboratory for dissemination to the science team members. Three automated stations are currently operational: one at Sondre Stromfjord, one at Tromso, Norway, and a third at Ft. Churchill, Canada.

PRELIMINARY BEACON RESULTS

The Sondre Stromfjord HILAT station became operational in September 1983; however, full operation did not start until late October. Figure 5 is a plot of the VHF signal intensity and phase scintillation and a map grid showing the trajectory of the pass that oc-

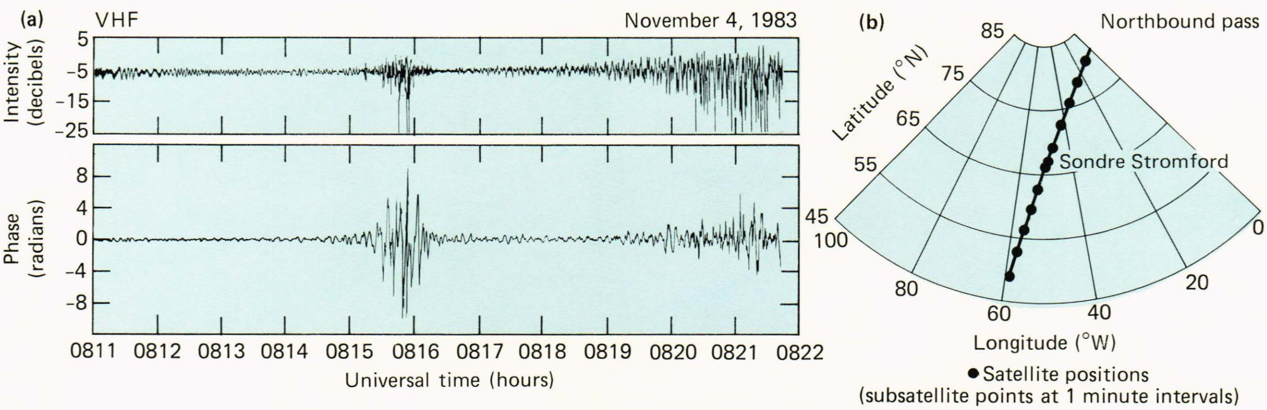

Figure 5—(a) Plot of detrended VHF signal intensity and VHF phase. (b) Map grid showing the south-to-north trajectory of the satellite.

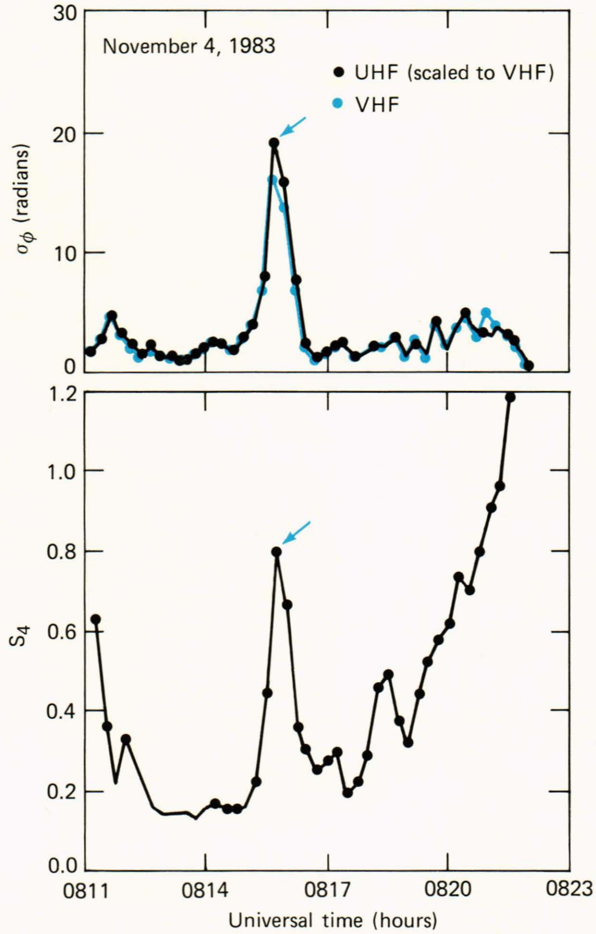

Figure 6—Amplitude and phase scintillation summary parameters. The arrows indicate the localized enhancement that is given in Fig. 8.

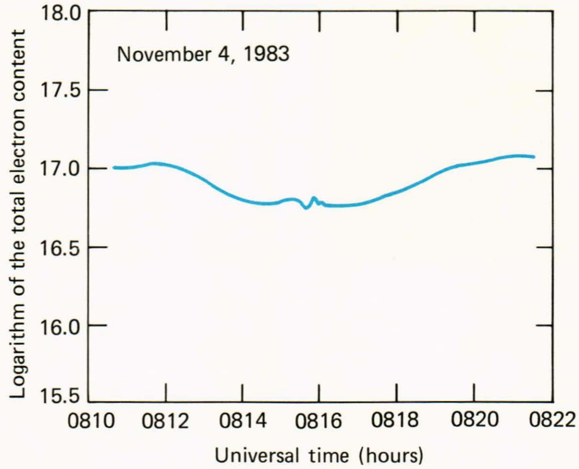

Figure 7—Total electron content derived from UHF phase data.

curred in the early morning local time sector. The event of primary interest is the burst of scintillation near the center of the pass. Such events are very common in the Sondre Stromfjord data and are believed to be associated with localized, highly structured F-region enhancements ("blobs"). For routine analysis, the data are summarized by moments, and spectra are computed on a "sliding" 30 second data window with outputs generated every 15 seconds. Figure 6 shows the scintillation summary parameters generated during the in-field data reduction. The UHF phase data have been scaled to VHF (using the theoretical linear wavelength dependence) to show the consistency of the data channels.

Figure 7 is a plot of the total electron content derived from the UHF signals. The systematic enhancement at the beginning and end of the pass is due to the changing slant range. For a uniform layer, the total electron content varies with the secant of the zenith angle. The localized total electron content enhancement near the center of the pass is coincident with the scintillation burst. Such an enhancement is consistent with an enhanced F region as the source.

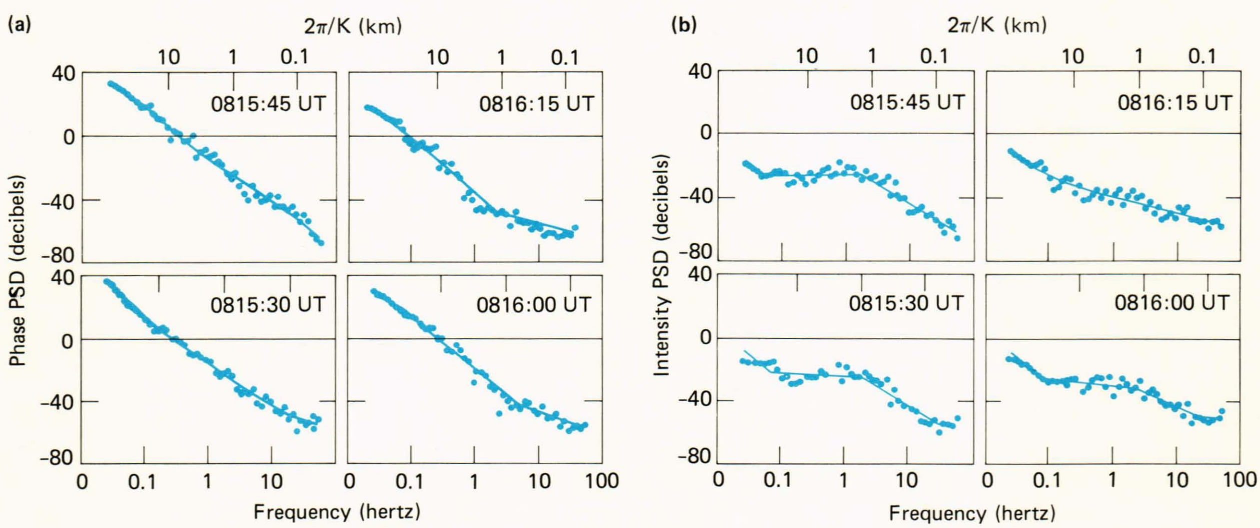

Figure 8—(a) Phase spectra measured within the local scintillation enhancement (November 4, 1983). (b) Intensity spectra corresponding to the phase spectra of (a). Note the suppression of low frequencies due to Fresnel filtering.

Figure 8 shows the four phase and intensity spectra through the scintillation burst obtained from the routine summary data. The spectra have been fitted to a multicomponent power law. The low-frequency suppression of the intensity spectra due to Fresnel filtering is clearly evident. The central portion of the phase spectra shows a power-law slope very near 3, but the spectra have a somewhat shallower high frequency segment. At the lowest frequencies the spectra remain enhanced.

The low-frequency enhancement in the phase spectra is possibly a feature imparted by the irregularity source that would be revealed by the particle detector data. In the next segment, structure is thought to be generated by a turbulence-like cascade. The drivers for this process may include both E fields and currents that are measured by HILAT instruments.

Finally, the highest frequency structure is strongly affected by crossfield diffusion, which is affected by a variety of ionospheric phenomena, particularly the presence of a conducting E layer. The unique complement of HILAT instrumentation will help sort out these various processes that affect the generation and decay of irregularities.